Development and Evaluation of a Hip Exoskeleton for Lateral Resistance Walk Exercise

Wujing Cao, Dongyang Shang, Meng Yin, Xinwei Li, Tiantian Xu, *Member, IEEE*, Li Zhang, *Fellow, IEEE*, and Xinyu Wu, *Senior Member, IEEE*

***Abstract*—Lateral resistance walk exercise (LRWE) is a popular method for fitness and rehabilitation training. However, current methods such as lateral band walks (LBW) cannot actively control the resistance training intensity. In this article, we proposed a novel hip exoskeleton, which can strengthen hip adductors by applying active resistance torque during lateral walking. The spatial linkage mechanism of the hip exoskeleton was designed and a prototype was fabricated. The dynamic model of transmission system coupling exoskeleton and human body was established. The proportional-integral-differential (PID) control strategy based on fuzzy tuning was presented to control the resistance torque. Physical prototype experiments showed that the fuzzy tuning PID control strategy could significantly improve the torque tracking accuracy compared to the traditional PID control strategy. The muscle activities of No-exo, Exo-off, LBW, and Exo-on (10 Nm, 15 Nm, 20 Nm) conditions were evaluated on ten healthy male subjects walking laterally at a speed of one step per second. The muscle activities of gluteus medius increased by 51.4%, 413.5%, 591.9%, 721.6%, and 918.9% under Exo-off, LBW, and Exo-on (10 Nm, 15 Nm, 20 Nm) conditions, respectively. The corresponding increments for tensor fasciae latae were 52.6%, 1136.8%, 1626.3%, 1994.7%, and 2331.6%, respectively. The results demonstrate that the proposed hip exoskeleton can apply to LRWE and improve muscle activities of hip adductors. It will upgrade the exercise method of LRWE and has good potential in strengthening hip abductors.**

***Index Terms*—Dynamic model, fuzzy tuning, hip exoskeleton, lateral resistance walk exercise, muscle activity.**

I. Introduction

LATERAL resistance walk exercise (LRWE) primarily targets and strengthens the hip abductors. This exercise improves people's flexibility and stability and helps prevent injuries [1]. The primary mover muscles of hip abductors are gluteus medius and tensor fasciae latae [2]. The glute medius assists with pelvic stability, flexion of the hips, and extension of the hips [3]. The tensor fasciae latae is a hip synergist muscle and allows glute gluteus medius and gluteus minimus to function with ease [4]. They are essential for helping keep the lower back straight, maintaining proper body alignment and coordinating dynamic body movements [5]. The primary rationale for prescribing the LRWE has been regarded as a key component in the prevention and rehabilitation of lower limb injuries [6], [7], and in the correction of undesirable movement patterns characterized by excessive femoral medial rotation and adduction [8].

Lateral band walks (LBW) is one of the most common rehabilitative exercises utilized by clinicians to strengthen the hip abductors [9], [10], as shown in Fig. 1(a). The method is using an elastic band secured around the lower extremities to provide resistance during lateral side stepping [11]. It is a simple and practical method. However, the training force cannot be active-controlled in a determined lateral walk process. It means the training is relative rough. The force control includes two parts. One is the action gait phase of the resistance force, the other is the magnitude. The trainer can choose different bands to change the intensity of training. However, it cannot control the action gait phase, which is important for the precise exercise of muscles. The forward walking is also limited when the band is on the people. Besides, it is impossible to provide constant resistance force with bands during training. To deal with abovementioned

Manuscript received 5 January 2023; revised 20 March 2023; accepted 23 April 2023. Date of publication 30 June 2023; date of current version 16 August 2023. Recommended by Technical Editor Z. Chen and Senior Editor Q. Zou. This work was supported in part by the National Natural Science Foundation of China under Grant 62125307 and Grant 62003327, in part by the NSFC-Shenzhen Robotics Research Center Project under Grant U2013207, in part by the Shenzhen Science and Technology Program under Grant JCYJ20220531100808018, in part by the Guangdong Basic and Applied Basic Research Foundation under Grant 2021A1515011699, and in part by SIAT-CUHK Joint Laboratory of Robotics and Intelligent Systems. *(Corresponding author: Xinyu Wu.)*

This work involved human subjects or animals in its research. Approval of all ethical and experimental procedures and protocols was granted by Medical Ethics Committee of Shenzhen Institute of Advanced Technology, Application No. SIAT-IRB200715-H051.

Wujing Cao, Meng Yin, Tiantian Xu, and Xinyu Wu are with the Guangdong Provincial Key Lab of Robotics and Intelligent System, Shenzhen Institute of Advanced Technology, Chinese Academy of Sciences, Shenzhen 518005, China, and also with the SIAT Branch, Shenzhen Institute of Artificial Intelligence and Robotics for Society, Shenzhen 518005, China (e-mail: wj.cao@siat.ac.cn; meng.yin@siat.ac.cn; tt.xu@siat.ac.cn; xy.wu@siat.ac.cn).

Dongyang Shang is with the Northeastern University, Boston, MA 02115 USA (e-mail: 2110095@stu.neu.edu.cn).

Xinwei Li is with the Shanghai Jiao Tong University, Shanghai 200240, China (e-mail: lixinwei0806@sjtu.edu.com).

Li Zhang is with the Chinese University of Hong Kong, Hong Kong (e-mail: lizhang@mae.cuhk.edu.hk).

This article has supplementary material provided by the authors and color versions of one or more figures available at https://doi.org/10.1109/TMECH.2023.3273717.

Digital Object Identifier 10.1109/TMECH.2023.3273717

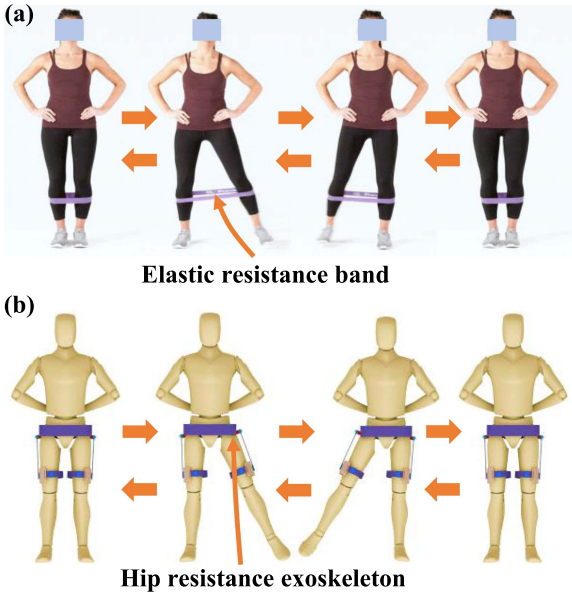

Fig. 1. (a) Lateral band walks. (b) Hip exoskeleton to provide resistance during lateral walking.

issues and upgrade the LRWE method, the portable intelligent device is needed to promote the intelligence of LRWE.

To the best of our knowledge, there is no wearable smart device for now which can be applied to LRWE directly. The similar devices are the hip exoskeletons, which have been developed for walking assistance [12], [13], [14], [15], [16]. These exoskeletons have demonstrated good performance in improving walking efficiency and reducing joint injuries. Hip exoskeletons may be applied to LRWE by providing resistance force instead of assistance force, as shown in Fig. 1(b). Some useful studies have been conducted in design, sensing and control of hip exoskeletons considering abduction-adduction torque [17]. Zhang et al. [18] developed a hip exoskeleton, which can assist walking and maintain balance in both the sagittal and frontal planes. However, the total weight of the hip exoskeleton excluding the battery unit is 9.2 kg, which is too heavy for the rehabilitation training. Yang et al. [19] presented a wearable soft robotic exosuit that applies a hip abduction torque and evaluate its ability to reduce knee adduction moment. Unfortunately, its target gait is still forward walking and the tension rope is not suitable for resistance. The exoskeleton named Gait Enhancing and Motivating System from Samsung Electronics has an additional passive joint at the hip for free abduction and adduction [20]. It cannot provide active force in the frontal plane. In a word, above hip exoskeletons [12], [13], [14], [15], [16], [18], [19], [20] are all developed for forward walking. The lateral walking gait is totally different with forward walking [21]. Transfer of gait detection methods and sensor strategies in forward walking to lateral walking has been limited. The control strategy for lateral walking resistance is still a lack of research. Therefore, challenges exist for development of a hip exoskeleton for lateral resistance walk exercise.

The aim of this article was to develop a hip exoskeleton for lateral resistance walk exercise and assess its performance by

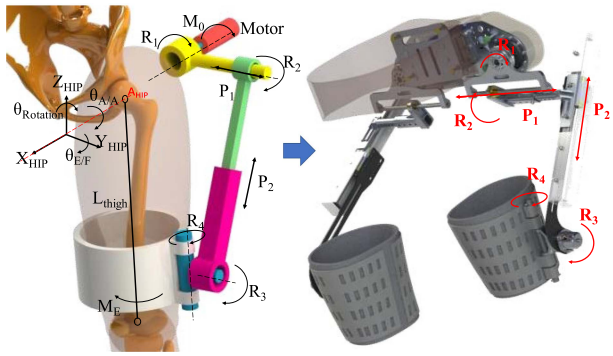

Fig. 2. Design and model of the hip exoskeleton.

muscle activity. For all we know, this is the first work that focuses on development and evaluation of a hip exoskeleton applied to lateral resistance exercise. The main contributions of this article are summarized as follows.

1) The first hip exoskeleton design and prototype to strengthen hip abductors during LRWE was presented. It provides an intelligent method for LRWE. The hip exoskeleton can actively provide constant resistance force in target lateral walking gait phase, which is impossible with bands.
2) The dynamic model of transmission system coupling exoskeleton and human body considering both transfer flexibility and nonlinear friction torque was established. Besides, the fuzzy tuning PID (FTPID) control strategy was presented to control the resistance torque. The torque tracking performance was enough for the LRWE.
3) The muscle activities of hip abductors including gluteus medius and tensor fasciae latae of leading leg under No-exo, Exo-off, LBW, and Exo-on (10 Nm, 15 Nm, 20 Nm) conditions were compared. The increments of gluteus medius and tensor fasciae latae show that the proposed hip exoskeleton is effective for the hip adductors strengthening during LRWE.

II. Methods

A. Structure and Prototype

The proposed design, illustrated in Fig. 2, is a spatial linkage mechanism that consists of four revolute joints and two prismatic joints (R1, P1, R2, P2, R3, R4). Simultaneously, the spatial linkage mechanism, respectively, provides one passive degree of freedom (DoF) for hip flexion/extension and hip internal/external rotation. It is significant to figure out the issue of axis alignment of human-robot coupling. The spatial linkage mechanism provides multi-DoFs to compensate deviation between the subject's hip joint and the motor output axis, and adapts the different body types of users. Meanwhile, the system translates motor torque M_0 at the revolute joint R_1 into a resistance torque M_E applied to the human thigh for hip abduction.

First, the spatial linkage mechanism adapts the real-time kinematic displacement and angular rotation of the axis of the subject's hip joint. When the exoskeleton is worn on subject,

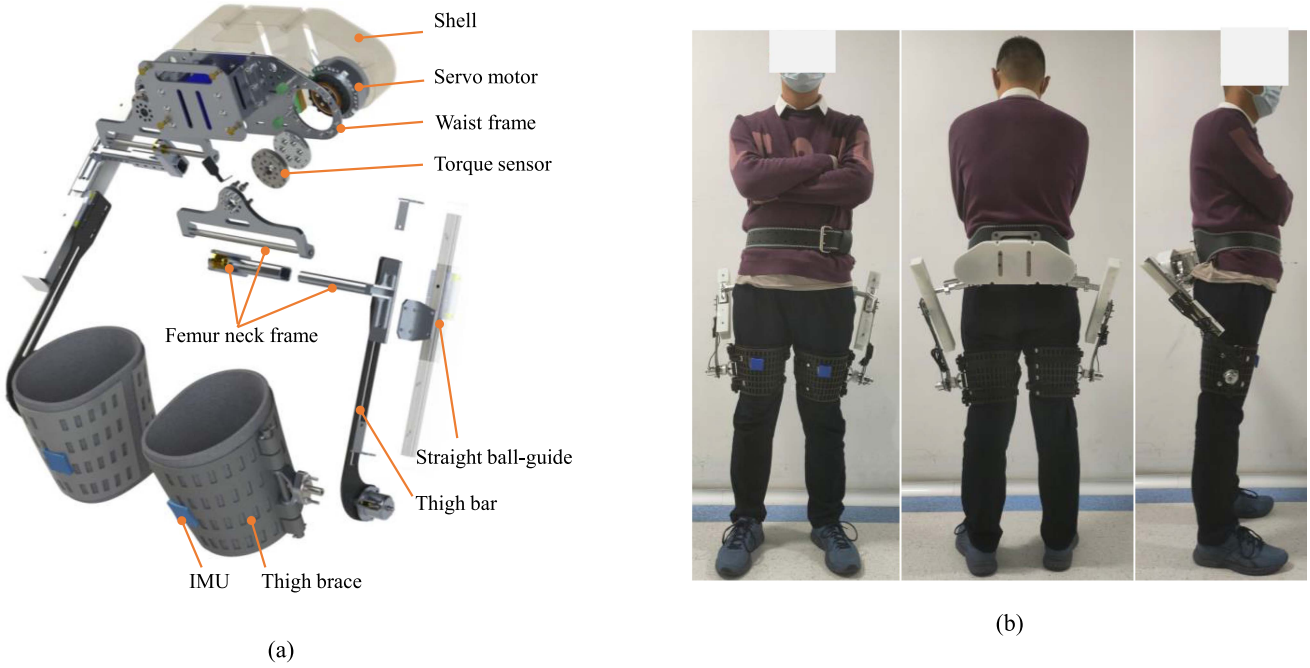

Fig. 3. (a) Detailed structures of the hip exoskeleton. (b) Prototype of the hip exoskeleton with a wearer.

the configuration of the joints of the spatial linkage mechanism is set and changing. The configuration changes according to the axis alignment deviation of human-robot coupling. To be specific, the real-time coordinate system of the instantaneous center of rotation of hip joint is defined in Fig. 2. The axis of hip abduction/adduction is A_{HIP} and the angular rotation of hip abduction/adduction named as $\theta_{A/A}$, which is corresponding to the angular rotation of motor R_1. To compensate the displacement deviation between the instantaneous center of rotation of hip joint and the output axis of motor in the front plane, the spatial linkage mechanism supplies prismatic degrees of freedoms P_1 and P_2, which corresponding to Y_{HIP} and Z_{HIP}, respectively. To compensate the angular displacement deviation between the axis A_{HIP} and the output axis of motor in the front plane, the spatial linkage mechanism provides rotational degrees of freedoms R_2 and R_3, which corresponding to $\theta_{E/F}$. In addition, the elasticity of the thigh brace and the rotational joint R_4 compensate the deviation from the $\theta_{rotation}$. By this function of real-time compensating deviation, this exoskeleton transmits the motor torque M_0 to the thigh of subject without axis alignment of human-robot coupling.

Second, the spatial linkage mechanism adapts the different body types between users. For example, for the subjects who have thicker or finer thighs, the joint P_1 slides more or less in the limited designed range. For the subjects who have longer or shorter thighs, the joint P_2 slides more in the limited designed range. To extend the range of the thigh width, the length of the femur neck frame is limited adjustable. For the subjects who have coxa vara or coxa valga, the initial angle of the joint R_1 changes to adapt. In a word, the designed motion range of the joints of the spatial linkage mechanism and the adjusting mechanism allow this exoskeleton to be adaptive to different users. The adjustment range of wearer's height is about 160–180 cm. The weight range is about 55–100 kg.

The detailed structures of the hip exoskeleton are shown in Fig. 3(a). We have uploaded the three-dimensional model file as supplementary material to make the detailed design of the exoskeleton available. The hip exoskeleton is fixed on the wearer by a hard cowhide leather belt with a waist frame. The control box and two servo motors (MBX70-50A-24V, MEBOTX, China) mounted on the waist frame can provide resistance torque up to 22 Nm. The weight of the motor is 0.68 kg, which is relative light compared to its rated torque. The shell adapts to the layout of the hardware and actuators and protects them. The hip exoskeleton structures of two sides are symmetrical. We give a description of its main structure by one side. A torque sensor connects the coupling and the femur neck frame. The straight ball-guide is connected to the femur neck frame and provides a DoF for linear displacement of thigh bar to compensate for wearing error and adapts to different thigh length. Abovementioned structures constitute the space bar mechanism, which have following advantages.

1) The enough range of the two prismatic joints permit the system automatically to adapt itself to different body types.
2) The remote center of rotation of the thigh brace is set approximatively at the instantaneous center of rotation of biological hip joint.
3) The obstruction and limit of the system to human are minimized during hip flexion/extension and hip internal/external rotation.

Two Inertial Measurement Units (IMUs, LPMS-B2, Alubi, China) placed on the thigh braces in front of the thigh are used to recognize the gait phases of lateral walking. A prototype

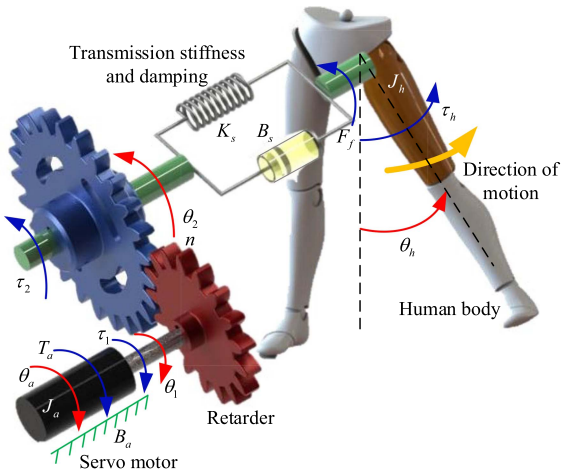

Fig. 4. Schematic diagram of the hip exoskeleton transmitting torque. Where T_a represents the electromagnetic torque generated by the servo motor; J_a represents the inertia of the servo motor; θ_a represents the rotation angle of the servo motor; B_a represents the rotational damping coefficient of the servo motor; τ_1 represents· the servo motor shaft torque, θ_1 represents the motor shaft rotation angle; n represents the reduction ratio of the reducer; θ_2 represents the output shaft angle of the reducer; τ_2 represents the output torque of the reducer; K_s represents the torsional stiffness of the transmission system; B_s represents the rotational damping coefficient of the transmission system; θ_h represents the hip joint angle; τ_h represents the driving torque of human hip joint; J_h represents the inertia of the human thigh; F_f is the friction torque.

of the hip exoskeleton was fabricated, as shown in Fig. 3(b). The total weight of the hip exoskeleton including the battery and electronics is about 5 kg. The waist frame and the femur neck frame are both made from 6061 Aluminum Alloy to meet stiffness requirement. The thigh bars are made of carbon fiber to decrease volume and weight of the hip exoskeleton. The most of the total mass is close to the center of mass of the wearer. This layout can reduce distal mass of the hip exoskeleton.

B. Dynamic Modeling of Transmission System Coupling Exoskeleton and Human Body

When the subject walks laterally with the proposed hip exoskeleton, the electromagnetic torque generated by the servo motor transmitted through the reducer increases the resistance of the human body. The resistance of the human body can be changed by adjusting the electromagnetic torque of the servo motor to achieve the effect of physical muscle training. The schematic diagram of the hip exoskeleton transmitting torque is shown in Fig. 4. Although the human body has considerable compliance, the lower limb was established as a rigid body in the model to reduce the complexity of modeling. In order to improve the compliance of human-exoskeleton coupling and the comfort of wearing, we added a spring-damping system to the exoskeleton.

According to the servo motor torque transmission theory, the dynamic equation of the servo motor in the hip exoskeleton can be obtained [14], as shown in

$$T_a = J_a\ddot{\theta}_a + B_a\dot{\theta}_a + \tau_1. \tag{1}$$

According to [22], the expression of the electromagnetic torque generated by the servo motor is shown in

$$T_a = 1.5p\left[\psi_f i_q + (L_d - L_q)i_d i_q\right] = 1.5\psi_f i_q = K_t i_q \tag{2}$$

where p is the pole pair number; Ψf is the flux produced by the rotor magnet, Ld and Lq are the equivalent inductances; i_d and i_q the currents in the direction of the magnet flux and the quadrature direction; and Kt is the torque coefficient.

In the design of the transmission system of the hip exoskeleton, the gearbox reducer is used to connect the servo motor and the human body. The reduction ratio of the gearbox is n. Thus, the rotation angle and torque transmission relationship of the reducer can be obtained, as shown in

$$\begin{cases} \theta_a = \theta_1 \\ \tau_2 = n\tau_1 \\ \theta_2 = \frac{1}{n}\theta_1. \end{cases} \tag{3}$$

Similarly, according to the torque transmission theory, (4) can be obtained

$$\begin{cases} \tau_2 = K_s\left(\theta_2 - \theta_h\right) + B_s\left(\dot{\theta}_2 - \dot{\theta}_h\right) \\ \tau_a = \tau_2 + F_f \end{cases} \tag{4}$$

where τ_a represents the resistance torque of human hip joint, which it resists the hip joint motion of the human body. It consists of two parts. One part is generated by the motor through the transmission system. The other part is friction torque.

The dynamic equation of human hip joint is shown in

$$\tau_h - \tau_a = J_h\ddot{\theta}_h. \tag{5}$$

By synthesizing (1)–(5), the dynamic equations of the hip exoskeleton transmission system can be obtained, as shown in

$$\begin{cases} T_a = K_t i_q = J_a\ddot{\theta}_a + B_a\dot{\theta}_a + \tau_1 \\ \tau_h - \tau_a = J_h\ddot{\theta}_h \\ \tau_1 = \frac{1}{n}\tau_a \\ \tau_a = K_s\left(\frac{1}{n}\theta_a - \theta_h\right) + B_s\left(\frac{1}{n}\dot{\theta}_a - \dot{\theta}_h\right) + F_f. \end{cases} \tag{6}$$

Among them, the friction torque in the hip exoskeleton dynamic equations can be represented by the LuGre model. Compared with the Coulomb friction model and the Stribeck friction model, the LuGre model can more clearly describe the mechanical behavior of friction torque. Especially, it has advantages in describing the stage from static friction to dynamic friction [23]. Its expression is shown in

$$\begin{cases} F_f = \chi_0 z + \chi_1\dot{z} + \chi_2\dot{\theta}_a \\ \dot{z} = \dot{\theta}_a - \varepsilon_0 z\left(\left|\dot{\theta}_a\right| \Big/ f\left(\dot{\theta}_a\right)\right) \end{cases} \tag{7}$$

where χ_0, χ_1, and χ_2 represent the parameters in the LuGre model; z represents the internal friction state; $f(\dot{\theta}_a)$ represents a Stribeck function [24], and its expression is shown in

$$f\left(\dot{\theta}_a\right) = F_c + (F_s - F_c)\exp\left[-\left|\dot{\theta}_a \Big/ \theta_s\right|^2\right] \tag{8}$$

where F_c and F_s represent the coulomb and static friction torque; θ_s represents the Stribeck speed. In the simulation process,

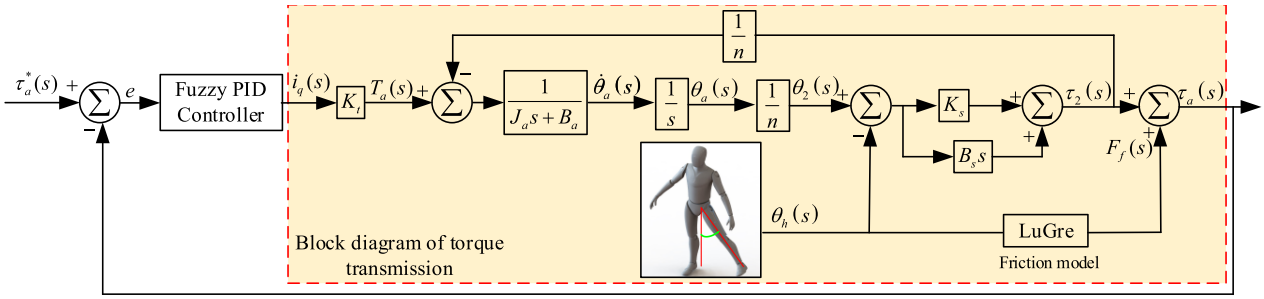

Fig. 5. Control block diagram of the hip exoskeleton.

parameters of the LuGre model are shown in our previous work [23].

According to (6), we can get the dynamic model of transmission system coupling exoskeleton and human body considering both transmission flexibility and nonlinear friction torque. The dynamic model reveals the coupling torque transmission relationship of human and the exoskeleton robot.

C. PID Control Strategy Based on Fuzzy Tuning

In order to stabilize the output resistance torque of the hip exoskeleton, this article uses the fuzzy tuning PID control strategy to control the output torque of the servo motor. The control block diagram is shown in Fig. 5.

The parameters of fuzzy tuning PID controller are adjusted in real time according to error, error variation law, and fuzzy rules [25]. Fuzzy tuning PID controller takes error and error variation law as input, and the PID controller parameters as output. The PID parameters are adjusted online according to fuzzy inference rules.

According to our previous work [26], the fuzzy domain of the PID controller's parameters is $[-6, 6]$. Similarly, the fuzzy domain of the error is $[-0.3, 0.3]$; the fuzzy domain of the error rate is $[-0.6, 0.6]$. The fuzzy subset of the fuzzy PID controller designed in this article is shown in

$$e, ec, \Delta k_p, \Delta k_i, \Delta k_d = \{\text{NB} \quad \text{NM} \quad \text{NS} \quad \text{O} \quad \text{PS} \quad \text{PM} \quad \text{PB}\} \tag{9}$$

where Δkp, Δki, and Δkd represent the output of fuzzy rules, respectively; e represents the resistance torque error; ec represents the error variation law of resistance torque error, and its expression is shown in

$$\begin{cases} e = \tau_a^* - \tau_a \\ ec = \dot{e} \end{cases}. \tag{10}$$

Specific output values of the PID controller parameters can be obtained according to fuzzy inference rules, as shown in

$$\begin{cases} K_p = K_{P0} + k_P \Delta k_P \\ K_i = K_{i0} + k_i \Delta k_i \\ K_d = K_{d0} + k_d \Delta k_d \end{cases} \tag{11}$$

where K_{p0}, K_{i0}, and K_{d0} represent the initial values of controller parameters; k_p, k_i, and k_d represent the proportional coefficients of the controller parameters.

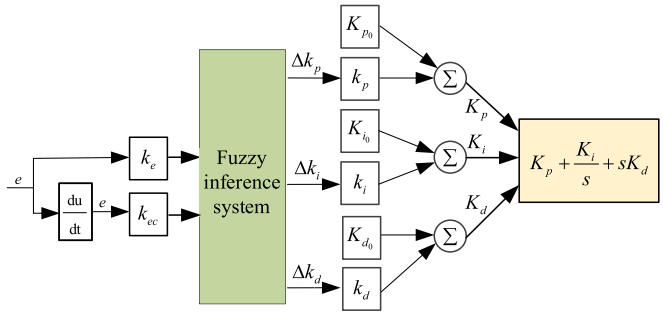

Fig. 6. Parameter calculation process of fuzzy tuning PID controller.

The specific expression is shown in

$$\begin{cases} k_P = \frac{K_{P\max} - K_{P\min}}{6} \\ k_i = \frac{K_{i\max} - K_{i\min}}{6} \\ k_d = \frac{K_{d\max} - K_{d\min}}{6} \end{cases} \tag{12}$$

where $K_{p\max}$, $K_{i\max}$, and $K_{d\max}$ represent the maximum value of controller parameters; $K_{p\min}$, $K_{i\min}$, and $K_{d\min}$ represent the minimum values of the controller.

The parameter calculation process of fuzzy tuning PID controller is shown in Fig. 6. According to Fig. 6, we know that the fuzzy rules can adjust the parameters of the PID controller in real time according to the error and error variation law. Thus, precise control of torque can be achieved during human movement. The distribution diagram of fuzzy input relationship is shown in Fig. 7. Fig. 7 shows the fuzzy tuning logic of PID parameters and the increment of controller parameters obtained according to the error and error variation law.

D. Human Subject Experimental Protocol

Ten healthy males (27±4 years old, 1.74±0.05 m, 70.2±9.1 kg) were recruited to validate the functional performance of the hip exoskeleton. All of them had no musculoskeletal problems that affect walking ability. The subjects were required to train three days to be acclimated to lateral walking and the hip exoskeleton. In the training session, they participated in 8 random lateral walking trails each of ten steps. The trials include lateral walking without wearing the hip exoskeleton (No-exo), lateral walking with the hip exoskeleton actively providing resistance (Exo-on), lateral walking with the hip exoskeleton unpowered (Exo-off), and lateral walking with a 20lb resistance

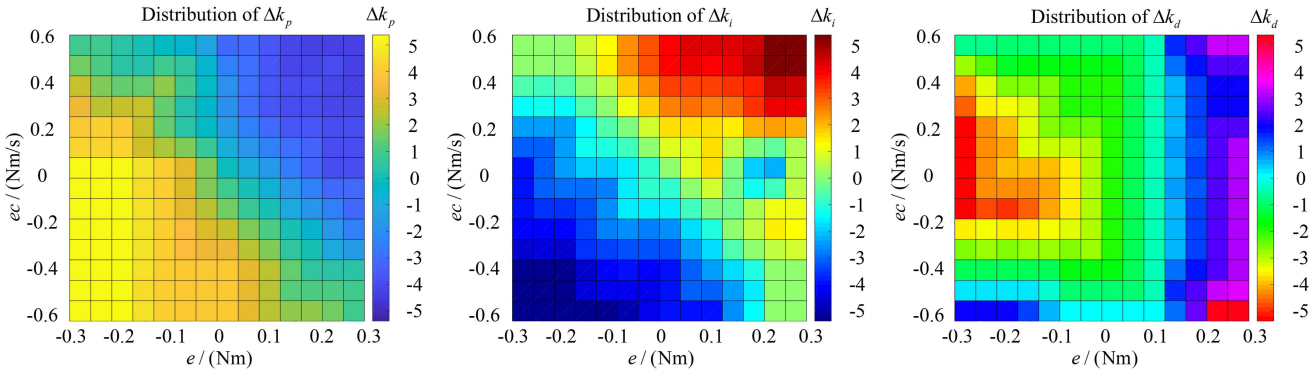

Fig. 7. Distribution diagram of fuzzy input relationship. (a) Distribution of Δk_p. (b) Distribution of Δk_i. (c) Distribution of Δk_d.

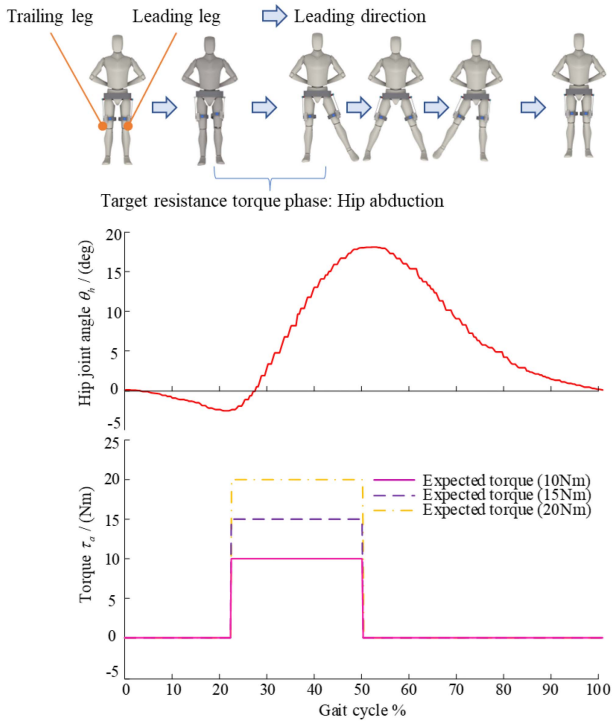

Fig. 8. Target resistance torque phase and expected resistance torques.

band (LBW). Each mode is experienced twice. The subjects were asked to rest for 5 min between every two cases of lateral walking. The elastic band resistance was chosen based on the recommendation of a professional fitness trainer. The resistance is especially helpful for beginners. Too much resistance makes it difficult to carry out the experiment, and too little resistance makes it difficult to be effective. An informed consent was signed for each subject prior to participate in the experiments. This article was approved by the Medical Ethics Committee of Shenzhen Institute of Advanced Technology (SIAT-IRB-200715-H0512).

The target motion of the exoskeleton is the hip abduction. The hip abduction phase of leading leg during lateral walking is about 23%–50% of the gait cycle. Thus, the hip abduction phase is the target resistance torque phase. The lateral walking gait and target resistance torque phase are shown in Fig. 8. Three

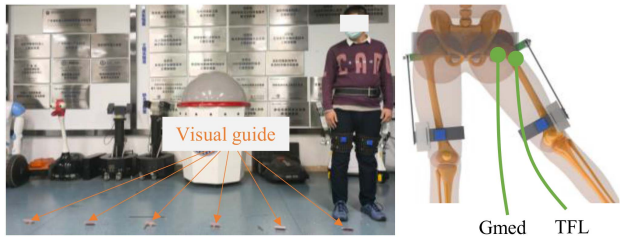

Fig. 9. Test scheme and position of the EMG electrodes. .

expected torques including 10 Nm, 15 Nm, and 20 Nm were set to represent different exercise levels.

The first experiment was to test the torque tracking performance of the controller. The torque sensor (M2210A2, Sunrise Instruments, China) was used to collect torque signals. Since the force tracking performance is similar for different people, we just asked one subject to walk laterally five steps in the leading direction. A visual guide, which utilizes pink cards to indicate each lateral step was placed on the floor to create a path for subjects to follow. The lateral step width between cards is 50 cm. Each subject was asked to walk five steps laterally to the right and repeat twice. The step frequency is set to be one step per second by a metronome. The interaction torque is measured by the torque sensor. The actual torques and errors of PID and FTPID control strategies during last two steps were presented.

The second experiment was to assess the effect of the hip exoskeletons on wearers in muscle activity. The test scheme and position of the electromyography (EMG) electrodes are shown in Fig. 9. The muscle activity of gluteus medius and TENSOR FASCIAE LATAE were recorded. The Biometrics PS850 system (Biometrics, Britain) is used to collect the myoelectric signals. The EMG data were sampled at a frequency of 1000 Hz. Raw EMG signals were band-pass filtered (20–460 Hz) in the electromyography system, rectified, and low-pass filtered (fourth-order Butterworth, cut-off frequency 6 Hz) in the software (MATLAB, Mathworks). Each of ten participants was asked to conduct four trials under different conditions. The trials include No-exo, Exo-on, Exo-off, and LBW. Each subject has a 30-min rest after each trial. The muscle activity was presented as a percentage of the maximum voluntary isometric contraction (% MVIC). The 100% MVIC of the gluteus medius and tensor

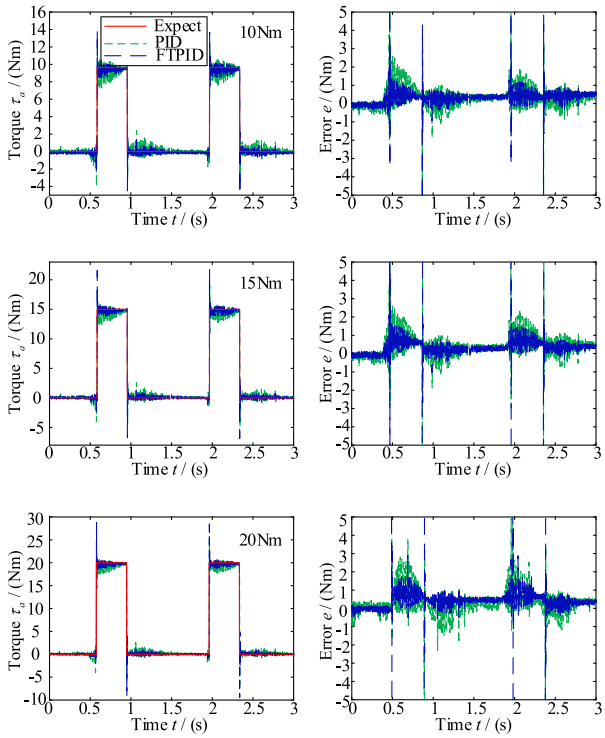

Fig. 10. Experimental results of physical prototypes with different control strategies.

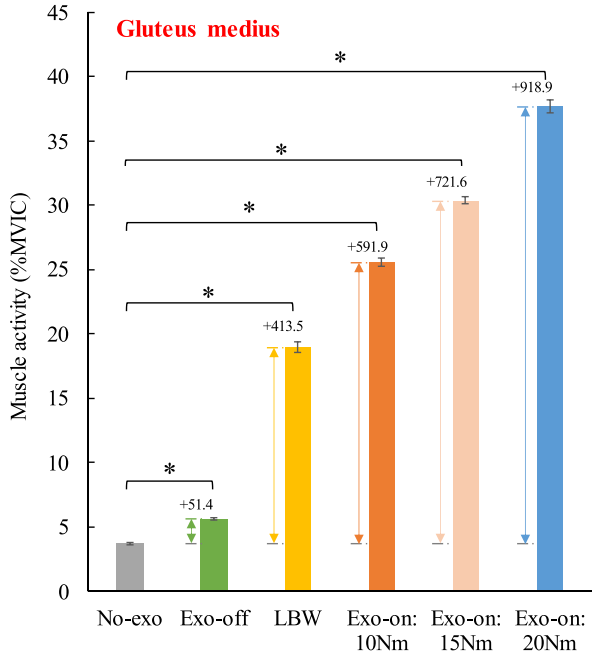

Fig. 11. Muscle activities of gluteus medius under different lateral walking conditions. Asterisks indicate statistically significant differences.

fasciae latae are measured according to [27]. EMG data collected during the target resistance torque phase were normalized to their muscles' respective MVIC trials and therefore expressed as % MVIC. The result of muscle activity is reported in the form of the mean ± standard error of the mean (SEM). The effects of different conditions on the muscle activity were analyzed using ANOVA. Differences among walking conditions were assessed using the two-sided paired *t*-tests.

III. Results and Discussion

A. Torque Tracking Performance of the Hip Exoskeleton

In order to verify the effectiveness of the proposed control strategy, the traditional PID and the fuzzy tuning PID control strategy are used, respectively, to carry out torque tracking experiments of the physical prototype. The results were shown in Fig. 10.

Fig. 10 shows the resistance torque tracking results obtained by the same subject moving under three different expected resistance conditions. The timing of the control experiment is consistent with two gait cycles. Although the resistance torque generated by the servo motor has the phenomenon of step overshoot, the tracking effect is gradually stable with the extension of control time. It can be seen from Fig. 10 that the fuzzy tuning control strategy proposed in this article can achieve stable tracking of the resistance torque and has smaller tracking errors. The variance of tracking error obtained by the PID control strategy is 0.0054, 0.0091, and 0.0135, respectively. However, the variance of tracking error obtained by the FTPID strategy is 0.0025, 0.0040, and 0.0068, respectively. The comparison shows the effectiveness of FTPID strategy. In addition, the FTPID control strategy has less adjustment time.

B. Muscle Activity

The muscle activities of gluteus medius in No-exo, Exo-off, LBW, and Exo-on (10 Nm, 15 Nm, 20 Nm) conditions were $3.7 \pm 0.1\%$MVIC, $5.6 \pm 0.1\%$MVIC, $19.0 \pm 0.4\%$MVIC, $25.6 \pm 0.3\%$MVIC, $30.4 \pm 0.3\%$MVIC, and $37.7 \pm 0.5\%$MVIC(mean ± SEM), respectively. The corresponding increments in the Exo-off, LBW, and Exo-on (10 Nm, 15 Nm, 20 Nm) conditions were 51.4%, 413.5%, 591.9%, 721.6%, and 918.9%, respectively (see Fig. 11). All the Exo-on modes increased the gluteus medius muscle activity compared to that No-exo, Exo-off, and LBW conditions. The increments of gluteus medius muscle activity were statistically significant ($P = 3.8E\text{-}23$, $P = 4.5E\text{-}24$, $P = 3.4E\text{-}23$) in all powered resistance modes compared to No-exo condition.

The muscle activities of tensor fasciae latae in No-exo, Exo-off, LBW, and Exo-on (10 Nm, 15 Nm, 20 Nm) conditions were $1.9 \pm 0.1\%$MVIC, $2.9 \pm 0.1\%$MVIC, $23.5 \pm 0.6\%$MVIC, $32.8 \pm 0.7\%$MVIC, $39.8 \pm 0.7\%$MVIC, and $46.2 \pm 0.7\%$MVIC(mean± SEM), respectively. The corresponding increments in the Exo-off, LBW, and Exo-on (10 Nm, 15 Nm, 20 Nm) conditions were 52.6%, 1136.8%, 1626.3%, 1994.7%, and 2331.6%, respectively (see Fig. 12). All the Exo-on modes increased the tensor fasciae latae muscle activity compared to that No-exo, Exo-off, and LBW conditions. The increments of tensor fasciae latae muscle activity were statistically significant ($P = 4.9E\text{-}20$, $P = 5.2E\text{-}21$, $P = 2.7E\text{-}22$) in all powered resistance modes compared to No-exo condition.

The major aim of this experiment is to verify that the hip exoskeleton can strengthen the hip abductors. The comparison

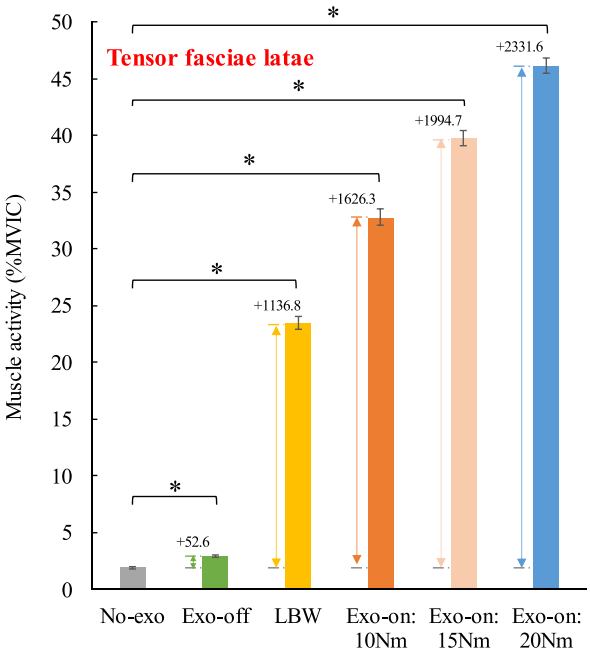

Fig. 12. Muscle activities of tensor fasciae latae under different lateral walking conditions.

of No-exo and Exo-on conditions is enough to verify its effectiveness in strengthening the hip abductors. Thus, the statistical comparisons were only made between the no-exo condition and the other conditions. The results of gluteus medius and tensor fasciae latae showed that the proposed exoskeleton can strengthen hip abductors. Several researchers have reported that the posture [28] and band position [29] have direct effect on the hip-muscle activity during resisted side stepping. An advantage of the hip exoskeleton is that it does not need to change position or posture to pursuit larger exercise intensity. What it needs is just increasing the resistance torque. In [28], the Gmed muscle activity of moving limb in upright standing posture is 18.7±8.0%MVIC, which is smaller than the Exo-on condition (10 Nm). In [29], the TFL muscle activity of moving limb with band on the ankle is about 20%MVIC, which is still smaller than the Exo-on condition (10 Nm). Besides, the hip exoskeleton can actively provide constant resistance force in target lateral walking gait phase, which is impossible with bands.

C. Limitations

Although the proposed hip exoskeleton has shown good performance in LRWE, a few of limitations of this article exist. The human body has considerable compliance that is not considered in coupling model of exoskeleton and human body. The compliance of human body should be researched in future work. The step width and speed are unchanging. Performance evaluation of the hip exoskeleton under different lateral walking speeds and step widths should be conducted. There is a room for reduction in the weight of the hip exoskeleton. Some components can be replaced by carbon fiber materials. Besides, the subjects are all healthy males. The effect of this hip exoskeleton on females and patients should be researched in following work.

IV. Conclusion

This article presents the design and prototype of a novel hip exoskeleton for LRWE. The dynamic model of transmission system coupling exoskeleton and human body was established. The FTPID control strategy was presented to control the resistance torque. The torque tracking performance of the proposed control strategy was evaluated and the muscle activity of hip abductors under different lateral walking modes were compared. The results demonstrate that the proposed hip exoskeleton can improve muscle activities of hip adductors. It will upgrade the exercise method of LRWE and has good potential in strengthening hip abductors. Metabolic cost is also an important index for exercise. We will conduct metabolic cost trials under different lateral walking conditions in the future work.

References

[1] C. Y. Kim, J. S. Lee, and H. D. Kim, "Comparison of the effect of lateral and backward walking training on walking function in patients with poststroke hemiplegia A pilot randomized controlled trial," *Amer. J. Phys. Med. Rehabil.*, vol. 96, no. 2, pp. 61–67, Feb. 2017.

[2] I. D. A. Paz et al., "Hip abduction machine is better than free weights to target the gluteus medius while minimizing tensor fascia latae activation," *J. Bodywork Movement Therapies*, vol. 30, pp. 160–167, Apr. 2022.

[3] P. Stastny et al., "Strengthening the gluteus medius using various bodyweight and resistance exercises," *Strength Conditioning J.*, vol. 38, no. 3, pp. 91–101, Jun. 2016.

[4] A. S. Klauser et al., "Intraobserver assessment of shear wave elastography in tensor Fasciae Latae and Gluteus Maximus muscle: The importance of the hip abductor muscles in runners knee compared to healthy controls," *J. Clin. Med.*, vol. 11, no. 13, pp. 1–9, Jul. 2022.

[5] P. H. Bauwens, I. Haidar, and M. Thaunat, "Endoscopic transfer of gluteus maximus and tensor fasciae latae for massive gluteus medius tear: Preliminary results," *Orthopaedics Traumatology -Surgery Res.*, vol. 107, no. 8, pp. 1–6, Dec. 2021.

[6] L. Chia et al., "Limited support for trunk and hip deficits as risk factors for athletic knee injuries: A systematic review with meta-analysis and best-evidence synthesis," *J. Orthop. Sports Phys. Ther.*, vol. 50, no. 9, pp. 476–489, Sep. 2020.

[7] Y. Omi et al., "Effect of hip-focused injury prevention training for anterior cruciate ligament injury reduction in female basketball players: A 12-year prospective intervention study," *Amer. J. Sports Med.*, vol. 46, no. 4, pp. 852–861, Mar. 2018.

[8] J. Dix et al., "The relationship between hip muscle strength and dynamic knee valgus in asymptomatic females: A systematic review," *Phys. Ther. Sport*, vol. 37, pp. 197–209, May 2019.

[9] L. J. Distefano et al., "Gluteal muscle activation during common therapeutic exercises," *J. Orthop. Sports Phys. Ther.*, vol. 39, no. 7, pp. 532–540, Jul. 2009.

[10] E. D. Cambridge et al., "Progressive hip rehabilitation: The effects of resistance band placement on gluteal activation during two common exercises," *Clin. Biomech.*, vol. 27, no. 7, pp. 719–724, Aug. 2012.

[11] H. B. O. Medeiros et al., "Hip torques and the effect of posture in side-stepping with elastic resistance," *Gait Posture*, vol. 93, pp. 119–125, Mar. 2022.

[12] Y. Qian, S. Han, Y. Wang, H. Yu, and C. Fu, "Toward improving actuation transparency and safety of a hip exoskeleton with a novel nonlinear series elastic actuator," *IEEE/ASME Trans. Mechatron.*, vol. 28, no. 1, pp. 417–428, Feb. 2023.

[13] T. Zhang, K. Feng, B. Zeng, and Z. Gong, "Design and validation of a lightweight soft hip exosuit with series-wedge-structures for assistive walking and running," *IEEE/ASME Trans. Mechatron.*, vol. 27, no. 5, pp. 2863–2874, Oct. 2022.

[14] S. Yu et al., "Quasi-direct drive actuation for a lightweight hip exoskeleton with high back drivability and high bandwidth," *IEEE/ASME Trans. Mechatron.*, vol. 25, no. 4, pp. 1794–1802, Aug. 2020.

[15] M. K. Ishmael, D. Archangeli, and T. Lenzi, "A powered hip exoskeleton with high torque density for walking, running, and stair ascent," *IEEE/ASME Trans. Mechatron.*, vol. 27, no. 6, pp. 4561–4572, Dec. 2022, doi: 10.1109/TMECH.2022.3159506.

[16] W. Cao, C. Chen, H. Hu, K. Fang, and X. Wu, "Effect of hip assistance modes on metabolic cost of walking with a soft exoskeleton," *IEEE Trans. Automat. Sci. Eng.*, vol. 18, no. 2, pp. 426–436, Apr. 2021.
[17] C. Siviy et al., "Opportunities and challenges in the development of exoskeletons for locomotor assistance," *Nature Biomed. Eng.*, vol. 7, pp. 456–472, Dec. 2022, doi: 10.1038/s41551-022-00984-1.
[18] T. Zhang, M. Tran, and H. Huang, "Design and experimental verification of hip exoskeleton with balance capacities for walking assistance," *IEEE/ASME Trans. Mechatron.*, vol. 23, no. 1, pp. 274–285, Feb. 2018.
[19] H. D. Yang, M. Cooper, A. E. Erdheim, D. Orzel, and C. J. Walsh, "A soft exosuit assisting hip abduction for knee adduction moment reduction during walking," *IEEE Robot. Autom. Lett.*, vol. 7, no. 3, pp. 7439–7446, Jul. 2022.
[20] Y. Pan et al., "Effects of bilateral assistance for hemiparetic gait post-stroke using a powered hip exoskeleton," *Ann. Biomed. Eng.*, vol. 51, no. 2, pp. 410–421, Feb. 2023.
[21] D. Yamashita et al., "Asymmetric interlimb role-sharing in mechanical power during human sideways locomotion," *J. Biomech.*, vol. 57, pp. 79–86, May 2017.
[22] Y. Chen, M. Yang, J. Long, K. Hu, D. Xu, and F. Blaabjerg, "Analysis of oscillation frequency deviation in elastic coupling digital drive system and robust notch filter strategy," *IEEE Trans. Ind. Electron.*, vol. 66, no. 1, pp. 90–101, Jan. 2019.
[23] D. Shang et al., "Dynamic modeling and fuzzy compensation sliding mode control for flexible manipulator servo system," *Appl. Math. Model.*, vol. 170, pp. 530–556, Jun, 2022.
[24] D. Shang, X. Li, M. Yin, and F. Li, "Vibration suppression for two-inertia system with variable-length flexible load based on neural network compensation sliding mode controller and angle-independent method," *IEEE/ASME Trans. Mechatron.*, vol. 28, no. 2, pp. 848–859, Sep. 2023.
[25] W. Zhong, X. Fu, and M. Zhang, "A muscle synergy-driven ANFIS approach to predict continuous knee joint movement," *IEEE Trans. Fuzzy Syst.*, vol. 30, no. 6, pp. 1553–1563, Jun. 2022.
[26] Y. Meng et al., "Mechanism and position tracking control of a robotic manipulator actuated by the tendon-sheath," *J. Intell. Robot. Syst.*, vol. 100, no. 3, pp. 849–862, Dec. 2020.
[27] J. W. Youdas et al., "Electromyographic analysis of trunk and hip muscles during resisted lateral band walking," *Physiotherapy, Theory Pract.*, vol. 29, no. 2, pp. 113–123, Feb. 2013.
[28] J. W. Berry et al., "Resisted side stepping: The effect of posture on hip abductor muscle activation," *J. Orthop. Sports Phys. Ther.*, vol. 45, no. 9, pp. 675–682, Sep. 2015.
[29] C. L. Lewis et al., "Hip-muscle activity in men and women during resisted side stepping with different band positions," *J. Athletic Training*, vol. 53, no. 11, pp. 1071–1081, Nov. 2018.

Wujing Cao received the Ph.D. degree in biomedical engineering from Rehabilitation Engineering and Technology Institute, University of Shanghai for Science and Technology, Shanghai, China, in 2019.

He is an Associate Research Fellow with Shenzhen Institute of Advanced Technology, Chinese Academy of Sciences. His research interests include lower limb exoskeleton and microprocessor-controlled prosthetic knee.

Dongyang Shang received the B.S. degree in mechanical design and automation from Shenyang Aerospace University, Shenyang, China, in 2018, and the M.S. degree in mechanical design and theory in 2021 from Northeastern University, Shenyang, China, where he is currently working toward the Ph.D. degree in mechanical engineering with the School of Mechanical Engineering and Automation.

His research interests include control theory and application and manipulator control with flexible joints.

Meng Yin received the Ph.D. degree in mechatronic engineering from State Key Laboratory of Robotics, Chinese Academy of Sciences, University of Chinese Academy of Sciences, Beijing, China.

He is currently a Postdoctoral Researcher with the Shenzhen Institutes of Advanced Technology, Chinese Academy of Sciences, Shenzhen, China. His research interest includes tendon-sheath driven humanoid robots.

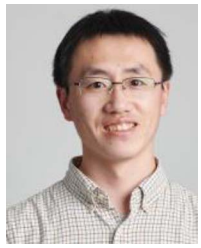

Xinwei Li received the Ph.D. degree in biomedical engineering from Rehabilitation Engineering and Technology Institute, University of Shanghai for Science and Technology, Beijing, China, in 2021.

He is currently a Postdoctoral Researcher with the Shanghai Jiao Tong University. His research interests include intelligent prosthesis and lower limb exoskeleton.

Tiantian Xu (Member, IEEE) received the M.S. degree in industrial engineering from École Centrale Paris, Gif-sur-Yvette, France, the Engineer degree (M.S.) in mechanic from Supméca, Saint-Ouen, France, in 2010, and the Ph.D. degree in robotics from the Institute of Intelligent Systems and Robotics, University of Pierre and Marie Curie, Paris, France, in 2014.

She was a Postdoctoral Fellow with the Department of Mechanical and Automation Engineering, The Chinese University of Hong Kong, Hong Kong, from 2014 to 2016. She is currently a Professor with the Shenzhen Institutes of Advanced Technology, Chinese Academy of Sciences, Shenzhen, China. Her research interests include currently focused on design and control of microrobots and lower limb exoskeletons.

Li Zhang (Fellow, IEEE) received the Ph.D. degree in physics from the University of Basel, Switzerland, in 2007.

In 2007, he was a Postdoctoral Fellow with the Institute of Robotics and Intelligent Systems, Swiss Federal Institute of Technology, Zürich, Switzerland, where he was a Senior Scientist from 2009 to 2012. He is currently an Associate Professor with the Department of Mechanical and Automation Engineering, The Chinese University of Hong Kong, Hong Kong. His main research interests include micro-/nanorobotics for biomedical applications and their collective behaviors.

Xinyu Wu (Senior Member, IEEE) received the B.E. degree in automation, M.E. degree in control science and engineering, and Ph.D. degree in automation and computer aided engineering from the Department of Automation, University of Science and Technology of China, Hefei, China, in 2001 and 2004, respectively.

He is currently a Professor with the Shenzhen Institute of Advanced Technology, Chinese Academy of Sciences, Beijing, China. He is the Director with the Center for Intelligent Bionic. His Ph.D. degree was awarded at the Chinese University of Hong Kong in 2008. He has authored and coauthored more than 180 papers and two monographs. His research interests include computer vision, robotics, and intelligent system.